Persistent luminescence properties of Cr^{3+}-Sm^{3+} activated $LaAlO_3$ perovskite

Yumiko Katayama,[1,*] Hiroaki Kobayashi,[1] Jumpei Ueda,[1] Bruno Viana,[2] and Setsuhisa Tanabe [1]

[1]*Graduate School of Human and Environmental Studies, Kyoto University, 606-8501 Kyoto, Japan*
[2]*PSL Research University, Chimie ParisTech – CNRS, Institut de Recherche de Chimie Paris, 75005 Paris, France*
[*]*katayama.yumiko.48a@st.kyoto-u.ac.jp*

Abstract: Deep red persistent luminescence properties of Cr^{3+} activated $LaAlO_3$ phosphors were investigated. The variation of lanthanide codopants, Sm^{3+}, Eu^{3+}, Tm^{3+} on thermoluminescence (TL) glow curves suggests an electron trap model of persistent luminescence in $LaAlO_3$:Cr^{3+} phosphors. Between lanthanide cations, Sm^{3+} was found to be a good codopant for enhanced persistent luminescence. TL excitation spectrum showed only UV bands similar to that of photoluminescence excitation which are attributed to $^4A_2 \rightarrow {}^4T_1(^4P)$. Based on the structure and intensity of TL glow curves after different wavelength excitation, it is found that the efficient charging through conduction band and inefficient local charging occur under UV and blue excitation, respectively.

OCIS codes: (160.2540) Fluorescent and luminescent materials; (090.2900) Optical storage materials; (160.6990) Transition-metal-doped materials; (170.3880) Medical and biological imaging.

References and links

1. T. Matsuzawa, Y. Aoki, N. Takeuchi, and Y. Murayama, "A new long phosphorescent phosphor with high brightness, $SrAl_2O_4$:Eu^{2+},Dy^{3+}," J. Electrochem. Soc. **143**(8), 2670–2673 (1996).
2. K. Van den Eeckhout, P. F. Smet, and D. Poelman, "Persistent luminescence in Eu^{2+}-doped compounds: A Review," Materials (Basel) **3**(4), 2536–2566 (2010).
3. K. Van den Eeckhout, D. Poelman, and P. D. Smet, "Persistent luminescence in non-Eu^{2+}-doped compounds: A Review," Materials (Basel) **6**(7), 2789–2818 (2013).
4. Y. Zhuang, Y. Katayama, J. Ueda, and S. Tanabe, "A brief review on red to near-infrared persistent luminescence in transition-metal-activated phosphors," Opt. Mater. **36**(11), 1907–1912 (2014).
5. Y. Katayama, J. Ueda, and S. Tanabe, "Effect of Bi_2O_3 doping on persistent luminescence of $MgGeO_3$:Mn^{2+} phosphor," Opt. Mater. Express **4**(4), 613–623 (2014).
6. T. Maldiney, A. Bessière, J. Seguin, E. Teston, S. K. Sharma, B. Viana, A. J. J. Bos, P. Dorenbos, M. Bessodes, D. Gourier, D. Scherman, and C. Richard, "The in vivo activation of persistent nanophosphors for optical imaging of vascularization, tumours and grafted cells," Nat. Mater. **13**(4), 418–426 (2014).
7. A. Bessière, S. Jacquart, K. Priolkar, A. Lecointre, B. Viana, and D. Gourier, "$ZnGa_2O_4$:Cr^{3+}: a new red long-lasting phosphor with high brightness," Opt. Express **19**(11), 10131–10137 (2011).
8. F. Liu, W. Yan, Y.-J. Chuang, Z. Zhen, J. Xie, and Z. Pan, "Photostimulated near-infrared persistent luminescence as a new optical read-out from Cr^{3+}-doped $LiGa_5O_8$," Sci. Rep. **3**, 1554 (2013).
9. J. Xu, J. Ueda, Y. Zhuang, B. Viana, and S. Tanabe, "$Y_3Al_{5-x}Ga_xO_{12}$:Cr^{3+}: A novel red persistent phosphor with high brightness," Appl. Phys. Express **8**(4), 042602 (2015).
10. A. M. Srivastava and M. G. Brik, "Crystal field studies of the Mn^{4+} energy levels in the perovskite, $LaAlO_3$," Opt. Mater. **35**(8), 1544–1548 (2013).
11. Y. Katayama, H. Kobayashi, and S. Tanabe, "Deep-red persistent luminescence in Cr^{3+}-doped $LaAlO_3$ perovskite phosphor for in vivo imaging," Appl. Phys. Express **8**(1), 012102 (2015).
12. P. Dorenbos, "The electronic level structure of lanthanide impurities in $REPO_4$, $REBO_3$, $REAlO_3$, and RE_2O_3 (RE = La, Gd, Y, Lu, Sc) compounds," J. Phys. Condens. Matter **25**(22), 225501 (2013).
13. A. J. Wojtoxicz, P. Szupryczynski, D. Wisniewski, J. Glodo, and W. Drozdowski, "Electron traps and scintillation mechanism in $LuAlO_3$:Ce," J. Phys. Condens. Matter **13**(42), 9599–9619 (2001).
14. A. Lecointre, A. Bessière, A. J. J. Bos, P. Dorenbos, B. Viana, and S. Jacquart, "Designing a red persistent luminescence phosphor: The example of YPO_4: Pr^{3+}, Ln^{3+} (Ln= Nd, Er, Ho, Dy)," J. Phys. Chem. C **115**(10), 4217–4227 (2011).
15. A. Bessière, S. K. Sharma, N. Basavaraju, K. R. Priolkar, L. Binet, B. Viana, A. J. J. Bos, T. Maldiney, C. Richard, D. Scherman, and D. Gourier, "Storage of visible light for long-lasting phosphorescence in chromium-doped zinc gallate," Chem. Mater. **26**(3), 1365–1373 (2014).

#257134 Received 11 Jan 2016; revised 21 Feb 2016; accepted 22 Feb 2016; published 1 Apr 2016

16. J. Ueda, P. Dorenbos, A. Bos, K. Kuroishi, and S. Tanabe, "Control of electron transfer between Ce^{3+} and Cr^{3+} in $Y_3Al_{5-x}Ga_xO_{12}$ host via conduction band engineering," J. Mater. Chem. C Mater. Opt. Electron. Devices **3**(22), 5642–5651 (2015).
17. J. Ueda, P. Dorenbos, A. J. J. Bos, A. Meijerink, and S. Tanabe, "Insight into the thermal quenching mechanism for $Y_3Al_5O_{12}:Ce^{3+}$ through thermoluminescence excitation spectroscopy," J. Phys. Chem. C **119**(44), 25003–25008 (2015).
18. A. Dobrowolska, A. J. J. Bos, and P. Dorenbos, "Electron tunnelling phenomena in YPO_4:Ce,Ln (Ln = Er, Ho, Nd, Dy)," J. Phys. D Appl. Phys. **47**(33), 335301 (2014).

1. Introduction

Persistent phosphors show delayed luminescence which continues several seconds to several tens of hours after ceasing excitation light. These materials have been developed for application for safety signs as well as *in vivo* imaging application [1–5]. For *in vivo* imaging application, red to near-infrared (NIR) persistent luminescence is required [1,2], because biological tissues have high transmittance in these wavelength regions. The advantage of persistent phosphors for imaging application is that the material is used after ultraviolet (UV) excitation before injection, which leads to higher signal to noise ratio due to the absence of autofluorescence from animal tissues [6]. Till now, several Cr^{3+} activated red to NIR persistent phosphors have been reported [7–9].

Cr^{3+} activated $LaAlO_3$ compound shows zero phonon lines (*R*-line, $^2E \rightarrow {}^4A_2$ transition) at 734 nm at longer wavelength compared with other well-known Cr^{3+} activated oxides, for instance 694 nm in Al_2O_3 and in $ZnGa_2O_4$. This nature is due to the small Racah parameters of Cr^{3+} in this perovskite structure [10, 11]. In previous study, we reported that $LaAlO_3:Cr^{3+}$ phosphors show deep-red persistent luminescence after UV light excitation. In addition, Sm^{3+} ion was found to be a good codopant for increasing the persistent luminescence intensity more than 35-fold [11]. However, we did not explain the detail charging and detrapping mechanism of persistent luminescence, and did not investigate the Cr^{3+} concentration dependence.

In this study, the (de)trapping carrier on the $LaAlO_3:Cr^{3+}$-Sm^{3+} is discussed by the difference of the TL glow curves in the $LaAlO_3:Cr^{3+}$ with different trivalent lanthanide ions, Ln^{3+} (Ln = Sm, Eu and Tm) and by comparing the vacuum referred binding energy (VRBE) diagram [12]. The TL glow curves by various charging excitation wavelength and persistent luminescence decay curves at different temperatures were analyzed for the mechanism of charging and detrapping processes. We concluded that there are two types of (de)charging processes of the efficient carrier transportation through the conduction band and the inefficient local carrier tunneling. We also report the optimized concentration of Cr^{3+} and Sm^{3+} for the persistent luminescence performance at ambient temperature.

2. Experimental

Three series of $LaAlO_3$ ceramics were prepared: a) Cr^{3+} singly doped $LaAlO_3$ with different Cr^{3+} concentration, b) Cr^{3+}-Sm^{3+} codoped materials with several Cr^{3+} concentrations, and c) Cr^{3+}-Ln^{3+} (Ln = Sm, Eu and Tm) codoped materials with fixed dopant concentrations. Compounds with compositions of $LaAl_{(1-x)}Cr_xO_3$ (x = 0.003, 0.005, 0.010, 0.020, 0.040), $La_{0.9995}Sm_{0.0005}Al_{(1-x)}Cr_xO_3$ (x = 0.001, 0.002, 0.003, 0.005), and $La_{0.9995}Ln_{0.0005}Al_{0.995}Cr_{0.005}O_3$ (Ln = Eu and Tm) were prepared by using a solid state reaction method. La_2O_3, Ln_2O_3 (Ln = Sm, Eu, Tm) (99.9%), Al_2O_3 (99.99%) and $Cr(NO_3)_3$ (99.9%) were used as starting materials. Powders were well mixed with $Cr(NO_3)_3$ solution in the presence of ethanol. The dried powders were pressed into pellets of 13 mm diameter and sintered at 1500 °C for 10 h under air atmosphere. La_2O_3 was used immediately after firing at 500 °C for 2 h because of its hydroscopic nature [11]. Sample structures were confirmed by X-ray diffraction and exhibit a single-phase perovskite structure. The Cr^{3+} concentrations in the series a) and b) were confirmed by EPR measurement and were found to be almost the same for the same nominal content.

Persistent luminescence spectra of the samples 10 sec after shutting off a 300 W xenon lamp (Asahi MAX302) excitation with an UV module (250 to 380 nm) were measured by a CCD detector (Ocean Optics QE65Pro). Persistent luminescence decay curves were recorded

#257134 Received 11 Jan 2016; revised 21 Feb 2016; accepted 22 Feb 2016; published 1 Apr 2016

using a silicon photodiode (Electro-Optical Systems S-025-H) after excitation by the xenon lamp for 5 min. TL glow curves from 140 K or 150 K to 600 K, with a heating rate of 10 K/min, were measured with the silicon photodiode which is the same detector used for decay curve measurements. The pellet was held in a vacuum chamber and excited by the xenon lamp with the UV module and with band pass filters with FWHM of 10 nm in the range from 254 nm to 420 nm for 10 min before measurement. Only for Cr^{3+}-Sm^{3+} codoped $LaAlO_3$, TL spectra were also recorded by the CCD detector. For the TL glow curves from 10 K to 600 K and decay curves at different temperatures, the luminescence was recorded by a CCD camera (Roper Scientific Pixis 100).

3. Results and discussions

Figure 1 shows TL glow curves of Cr^{3+}:$^2E \rightarrow {}^4A_2$ deep red luminescence in the range from 150 K to 450 K for the Cr^{3+} singly doped and Cr^{3+}-Ln^{3+}(Ln = Sm, Eu and Tm) codoped $LaAlO_3$ samples. The Cr^{3+} singly doped sample shows a broad TL band from 150K to 380 K with a relatively sharp peak approximately at 200 K, while Sm^{3+} and Tm^{3+} codoped samples show additional TL peaks at around 350 K and at 270 K, respectively. On the other hand, Eu^{3+} codoped sample does not show any additional TL peak up to 450 K. Generally, TL peak in the range of 250 K to 350 K could result in long persistent luminescence at ambient temperature. Indeed, Sm^{3+} codoped sample showed the strongest persistent luminescence in a series of the lanthanide codoped materials tested for their perovskite compounds. The persistent luminescence intensity 10 min after stopping excitation light of Tm^{3+} and Eu^{3+} codoped material was of order 10^{-3} mW/Sr/m^2 whereas Sm^{3+} codoped sample showed higher intensity over one order of magnitude. The TL result is consistent with the result of the persistent luminescence intensity.

These results suggest that the persistent luminescence mechanism of Cr^{3+} doped $LaAlO_3$ phosphors follows electron-trap model. For Cr^{3+} singly doped material, the potential origins of electron traps may be oxygen vacancies, some impurities from raw materials and Cr ions. On the other hand, the origins of additional peaks with lanthanide codoping are probably from the electron traps by Ln^{3+}-related defects. The additional TL glow curve peak by Sm^{3+} codoping appears at higher temperature than that by Tm^{3+} codoping. If the traps created by lanthanide codoping have similar frequency factors, for instance $s = 1.0 \times 10^{13}$ s^{-1} which is the same order with the frequency factor of $LuAlO_3$ perovskiste at ambient temperature [13], trap depth E_{trap}(Ln) is 0.91 eV for Sm^{3+} and 0.69 eV for Tm^{3+} codoped sample. E_{trap}(Sm) is deeper than E_{trap}(Tm) (E_{trap}(Sm)> E_{trap}(Tm)). These trend can be explained by the VRBE model if the electron trap level is regarded as $Ln^{3+} + e^-$ or Ln^{2+} [12, 14]. The energy gaps ($E_{Ln2+-CB}$) between the ground state of Ln^{2+} ions and the bottom of conduction band referring to the VRBE diagram of the $LaAlO_3$ lattice is 0.75 eV for Tm, 1.22 eV for Sm and 2.47 eV for Eu, which are the values at low temperature (~10 K) (Fig. 2 (b)) [12]. The trend of the $E_{Ln2+-CB}$ between Sm and Tm is in agreement with that of the trap depths obtained from TL results (E_{trap}(Sm)> E_{trap}(Tm)). Taking into account the conduction band energy shifting with temperature, the $E_{Ln2+-CB}$ at 300 K is much similar to the E_{trap}(Ln) estimated from TL peak temperature. For the Eu^{3+} codoping sample, the TL peak temperature is estimated to be approximately 800 K from the $E_{Ln2+-CB}$ in the VRBE diagram, so that the corresponding TL peak was not observed in the TL glow curve up to 450 K. From these results, it was suggested that the persistent luminescence in $LaAlO_3$:Cr^{3+}-Sm^{3+} is caused by the electron trapping and detrapping to and from the Sm^{3+}-related defects.

To investigate the charging process, TL excitation (TLE) spectrum was measured as shown in Fig. 2(a). For the TLE spectrum, the TL glow curves by different charging wavelength were measured, normalized curves are shown in Fig. 2(b), and the integrated intensity of TL glow peaks in the range between 160K and 500K were plotted as a function of charging wavelength. The TLE spectrum shows two bands peaking at 270 nm and 350 nm, which are attributed to Cr^{3+}:$^4A_2 \rightarrow {}^4T_1(^4P)$ and probably due to the metal to metal charge transfer. Compared with PLE, TLE spectrum presents a red shift which may be due to a

#257134 Received 11 Jan 2016; revised 21 Feb 2016; accepted 22 Feb 2016; published 1 Apr 2016

vicinity to the conduction band. In that case as reported in other compounds [15], charges escape could occurs at lower energies. On the other hand, the band due to the $^4A_2 \rightarrow {}^4T_1(^4F)$ was not observed in the TLE spectrum. The efficient charging under below 350nm excitation suggests that the electron transportation occurs through the conduction band from the Cr^{3+} to Sm^{3+} because in general the charging occurs through the conduction band in persistent phosphors [16, 17]. Based on these results, we roughly assumed that photo-ionization threshold of Cr^{3+} is 350 nm (3.54 eV), and plotted the ground state of the Cr^{3+} state by subtracting photoionization threshold energy from the VRBE of conduction bottom (See VRBE diagram shown in Fig. 1(b)). In the TL glow curve shown in Fig. 2(b), two bands peaking approximately at 250 K and 350 K were observed. When the charging wavelength becomes much longer, the shallower electron trap at 250 K becomes relatively weaker compared with the peak at 350K. This difference of TL glow curves can be explained by the different charging process. In the excitation from 350nm to 420nm, Cr^{3+} is excited to the $^4T_1(^4F)$ state, which is approximately 1 eV below the conduction bottom. It is reported that, in $Y_3Al_5O_{12}:Ce^{3+}$, 1 eV gap between Ce^{3+} 5d excited state and the conduction bottom of the host lattice is not sufficient for photo-ionization at room temperature [17]. This can be adopted for $LaAlO_3:Cr^{3+}$, under $^4T_1(^4F)$ blue excitation, it is difficult to charge electrons into traps by photo-ionization and thermally assisted photo-ionization process through the conduction band. Therefore, charging process under blue excitation is probably due to tunneling process while that under UV excitation is through the conduction band. In our material, only 0.05% Sm works well as electron traps for persistent luminescence, which is quite low concentration for other lanthanide-ion-codoped persistent phosphors for tunneling [1, 18]. However, it is worth to mention that the TL intensity by 420 nm excitation is 180 times weaker than that by 270 nm excitation. Thus, small amount of Cr^{3+}-Sm^{3+} pairs could exist and show the tunneling process.

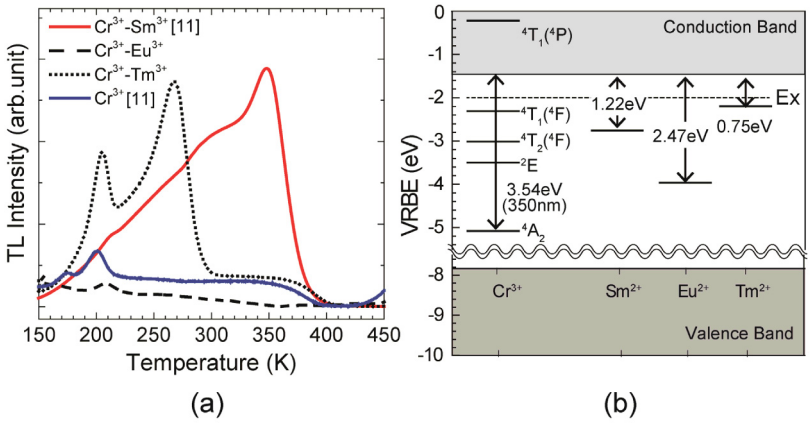

Fig. 1. (a) TL glow curves of $LaAlO_3$:0.5%Cr^{3+} and $LaAlO_3$:0.5%Cr^{3+}-0.05%Ln^{3+} (Ln = Sm, Eu, Tm) monitoring deep-red Cr^{3+} luminescence (TL glow curves of $LaAlO_3:Cr^{3+}$ and $LaAlO_3:Cr^{3+}$-Sm^{3+} are from ref [11].) and (b)VRBE energy diagram for Cr^{3+} and three lanthanide divalent ions. The VRBE values of band edges and ground state divalent lanthanide ions were adopted from ref [12]. Ex represents excitonic level which is 0.5 eV below the conduction bottom according to the VRBE model.

#257134 Received 11 Jan 2016; revised 21 Feb 2016; accepted 22 Feb 2016; published 1 Apr 2016

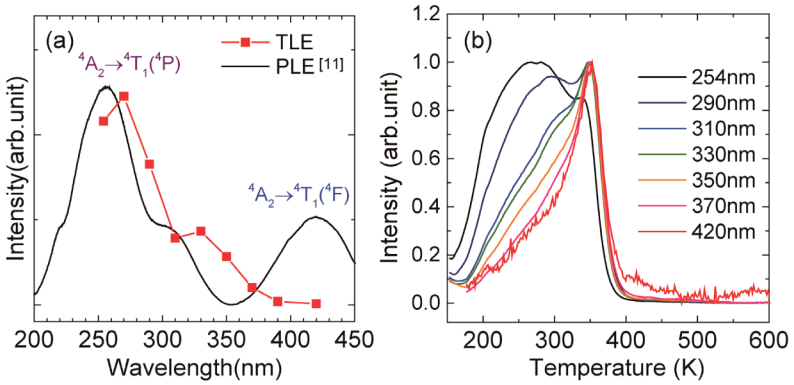

Fig. 2. (a) Themoluminescence excitation spectra of the $LaAlO_3$:0.5%Cr^{3+}-0.05%Sm^{3+} (closed-square line) and PLE spectra of the $LaAlO_3$:0.5%Cr^{3+} at ambient temperature from ref [11]. (solid curve). (b)Thermoluminescence glow curves of the $LaAlO_3$:0.5Cr^{3+} –0.05%Sm^{3+} after different wavelength irradiation from 254 nm to 420 nm with heating rate of 10 K/min.

When TL glow curve was measured just after stopping excitation light, significant increase in baseline below 200 K (Fig. 3) was observed. In addition, long persistent luminescence was observed at low temperature at 10 K and 100 K with the reciprocal intensity versus time presenting linear behavior (Fig. 3 inserted). These results indicate there is strong athermal tunneling detrapping process in this material.

The persistent luminescence mechanism of $LaAlO_3$:Cr^{3+}-Sm^{3+} can be commented by an electron trapping model as follows. Under UV excitation, efficient electron charging occurs from Cr^{3+} to the traps, probably through the conduction band. In case of blue excitation, weak TL was observed originating only for deeper traps. Therefore, charging process under lower energy blue excitation is probably through athermal process to the defect centers nearby Cr^{3+}. In the recombination process, both tunneling and thermally activated processes occur in this material.

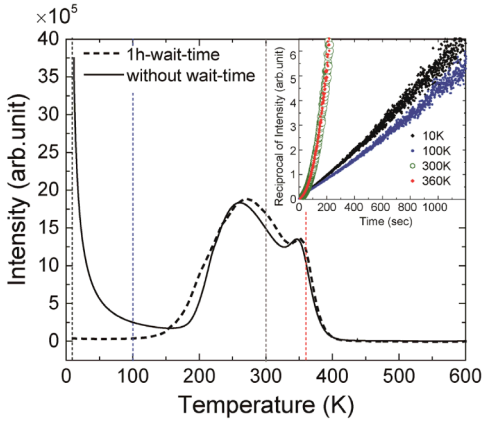

Fig. 3. Thermoluminescence glow curves of the $LaAlO_3$:0.5Cr^{3+} –0.05%Sm^{3+} just after low temperature 254 nm excitation (solid curve) and 1h after excitation (dashed curve). Inserted figure shows reciprocal persistent luminescence intensity as a function of time at 10 K, 100 K, 300 K and 360 K.

To find the optimum concentration of dopants for persistent luminescence intensity, Cr^{3+} singly doped and Cr^{3+}-Sm^{3+} codoped $LaAlO_3$ with several concentrations were prepared and the persistent luminescence intensity of the samples was examined. In Fig. 4(a), persistent luminescence intensities 10 min after stopping UV excitation are plotted as a function of Cr content. By X-band EPR measurement, no difference between the evolution of the Cr^{3+}/Sm^{3+}

#257134 Received 11 Jan 2016; revised 21 Feb 2016; accepted 22 Feb 2016; published 1 Apr 2016

content from nominal to actual values is observed as seen in Fig. 4(b). Sm^{3+} concentration of 0.05% was selected because this gives better persistent luminescence intensity than with 0.10% and 0.15%. Compared with the Cr^{3+} singly doped samples, the Sm^{3+} codoped samples show much higher persistent luminescence intensity. Both series of materials show first increase in low Cr^{3+} content and then shows decrease of the persistent luminescence intensity with increasing Cr^{3+} content. The optimal Cr^{3+} concentration is different for the two systems, 1.0% for Cr^{3+} singly doped materials and 0.5% for Cr^{3+}-Sm^{3+} codoped materials.

The difference in the optimum Cr^{3+} concentration is probably due to the higher defect concentration or energy migration through Sm^{3+} when Sm^{3+} is introduced in the compounds. It is obvious that the electron trap was changed from the intrinsic defects (oxygen vacancies, some impurities from raw materials and Cr ions) to Sm^{3+}-related defects and the trap concentration in Sm^{3+} codoped sample is much higher than that in Cr^{3+} singly doped materials (Fig. 4). Therefore, the average distance between Cr^{3+} emitting center and defects in the Cr^{3+}-Sm^{3+} codoped sample is much shorter than that in Cr^{3+} singly doped sample in the situation of the same Cr^{3+} concentration.

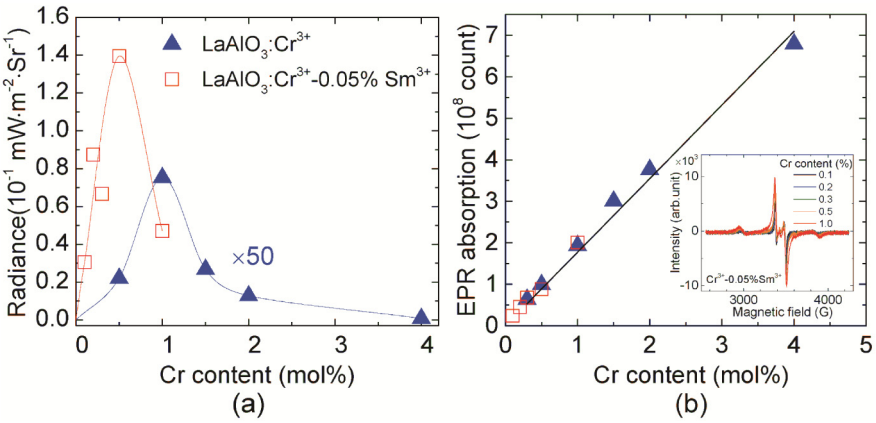

Fig. 4. Cr^{3+} content dependence of (a) persistent luminescence intensity 10 min after ceasing excitation light and (b) EPR absorption intensity. Inserted figure shows EPR spectra of Cr^{3+}-Sm^{3+} codoped sample. Notice that the intensity of $LaAlO_3$:Cr^{3+} in Fig. 4(a) is 50 times less than those of $LaAlO_3$:Cr^{3+}-Sm^{3+}.

4. Conclusion

Deep red persistent luminescence properties of Cr^{3+} activated $LaAlO_3$ phosphors were investigated. TL glow curves of lanthanide codoped sample showed additional peaks at 270 K by Tm codoping and at 350 K for Sm codoping. The TL result can be well explained by VRBE model and suggests electron trap model of persistent luminescence in $LaAlO_3$:Cr^{3+}-Ln^{3+}. Sm^{3+} was found to be a good codopant for strongly increasing persistent luminescence intensity. The optimized concentration for dopants were 0.5% for Cr^{3+} and 0.05% for Sm^{3+}. The structure of TL glow curve varied with different excitation wavelength, suggesting efficient persistent luminescence process through Cr^{3+} excited level inside the conduction band in the case of UV excitation and inefficient local charging and decharging process occurs after blue excitation.

Acknowledgments

We would like to acknowledge Dr. Yann Le Du for experimental support for EPR measurement. This work was financially supported by a Grant-in-Aid for Scientific Research from JSPS Fellows (No.26-40075).

#257134 Received 11 Jan 2016; revised 21 Feb 2016; accepted 22 Feb 2016; published 1 Apr 2016